8-25-2021

Juvenile Body Mass Estimation from the Femur Using Postmortem Computed Tomography Data

Laure Spake
University of Otago

Julia Meyers
University of Otago

Hugo F.V. Cardoso
Simon Fraser University

Juvenile Body Mass Estimation from the Femur Using Postmortem Computed Tomography Data

Laure Spake,[1,2]* Julia Meyers,[2] and Hugo F. V. Cardoso[3]

[1]Religion Programme, Department of Theology & Religion, University of Otago, Dunedin, New Zealand.

[2]Center for Research on Evolution, Belief, and Behavior, University of Otago, Dunedin, New Zealand.

[3]Department of Archaeology, Simon Fraser University, Burnaby, B. C., Canada.

*Correspondence to: Laure Spake, University of Otago, Religion Programme and Centre for Research on Evolution, Belief, and Behaviour, PO Box 56, Dunedin 9054 New Zealand. Email: laure.spake@otago.ac.nz.

Short Title: Juvenile Body Mass Estimation from the Femur

KEY WORDS: SKELETAL ESTIMATION, GROWTH AND DEVELOPMENT, POPULATION VARIATION, BIOLOGICAL PROFILE.

Abstract

Skeletal estimation methods to reconstruct the juvenile biological profile are largely limited to those estimating age, and to a lesser extent, sex. While body mass is not generally estimated as part of the biological profile in forensic investigations, this is a logical candidate for inclusion in the forensic biological profile, as it has long been of interest in paleoanthropology and several methods to estimate juvenile body mass currently exist. To explore the performance of body mass estimation for juveniles, we test the accuracy and precision of previously published panel regression formulae using two femoral measurements: the breadth of the distal metaphysis and the cross-sectional polar moment of inertia (*J*). The test sample consists of measurements of 94 individuals aged birth to 12.5 years, taken from post-mortem computed tomography scans housed at the Office of the Medical Investigator, New Mexico, USA. Results indicate that body mass estimates are more accurate when estimated from cross-sectional rather than metaphyseal measures. Both formulae, however, consistently underestimate weight, and the magnitude of the underestimation increases exponentially with age. This suggests that contrary to what others have argued, body mass estimation is complicated by population variation in body composition. This study reinforces the importance of documenting and investigating the ontogeny of human variation. The global increase in medical imaging in clinical settings can be leveraged to obtain skeletal data for juveniles from a wide range of ontogenic environments, marking an exciting time for the study of human variation.

Skeletal estimation methods for reconstructing the biological profile of juveniles have largely been focused on age estimation. While attempts have been made to estimate sex from the dentition (e.g. Black 1978; De Vito and Saunders 1990; Teschler-Nicola et al., 1998; Cardoso, 2008; Macaluso, 2011; Hasset, 2011; Viciano et al. 2011, 2013, 2020) and the skeleton (e.g. Weaver 1980; Schukowski 1993; Molleson and Cruse 1998; Wilson et al. 2008; Stull et al. 2017), these methods typically fall well short of the 90% accuracy rates traditionally expected of adult sex estimation methods (Mittler and Sheridan, 1992; Sutter, 2003; Scheuer, 2002; Cardoso and Saunders, 2008; Vlak et al., 2008; Cardoso 2010; Wilson et al., 2011; O'Donnell et al., 2017). There have been some attempts to develop methods for ancestry estimation (Buck and Strand Vidarsdóttir 2004) and stature estimation (Telkk et al. 1962; Feldesman 1992; Smith 2007) for juveniles, but largely, these aspects of the juvenile biological profile remain under studied. This gap in research concerning biological profile estimation for juveniles is partly the result of a lack of skeletal samples with enough juvenile individuals to capture a reasonable range of variation (Lewis and Rutty 2003).

In the last decade, however, juvenile skeletal data has become increasingly available for study. While new and large collections of juveniles are being established (e.g. Cardoso 2006; Alemán et al. 2012; Belcastro et al. 2017; Cattaneo et al. 2018), the bulk of new data has resulted from the global increase in availability and quality of medical imaging. Medical images from computed tomography (CT) scans are the most popular because the modality is particularly well suited to imaging dense tissues like bones and teeth. CT is routinely used for diagnostics in hospitals, dental offices, and now also in several post-mortem institutions around the world. Researchers have also studied scans resulting from magnetic resonance imaging (MRI), particularly for age estimation in the living because MRI avoids the patient radiation dose concerns of x-ray and CT imaging (e.g. Schmidt et al. 2007; Fan et al. 2016; Serin et al 2016). Others have used Lodox scans to collect skeletal measurements (e.g. Stull et al. 2014). For the first time and thanks to increasingly quick technological improvements, forensic anthropologists are able to capitalize on the virtual skeletal collections first proposed more than a decade ago (Grabherr et al. 2009).

While body mass estimation is not typically considered part of the biological profile in children, it is a good candidate for development relative to ancestry and stature estimation because it has been of interest in paleoanthropological and bioarchaeological contexts for some time. Forensic methods for estimating body mass can therefore build from the foundation established by paleoanthropologists (see Ruff and Niskanen 2018 for a review of studies concerned with juvenile body mass estimation). Because of paleoanthropological interest, there are several methods already available to estimate body mass in juveniles, and which have been argued to be applicable for forensic contexts. Estimation of body mass may be particularly useful to identify individuals at the extremes of variation whose unusual weight may be more likely to be reported to investigators. This is potentially a key difference between paleoanthropological and forensic uses of body mass estimation, because paleoanthropologists may be more interested in typical body weight variation. Understanding the performance of existing methods across different and diverse samples will provide a better picture of their potentials and pitfalls. In particular, testing the accuracy of these methods on independent samples will inform researchers and practitioners about whether these methods are reliable and useful for use in forensic settings.

The two most widely used juvenile body mass estimation methods were developed by Ruff (2007) and Robbins and colleagues (2010). Ruff's method (2007) consists of an equation that uses the distal femoral metaphyseal breadth, while Robbins and colleagues' method (2010) uses the femoral midshaft cross-sectional measure *J*. Both of these methods require that age first be estimated from dental development, and that either the distal femoral metaphyseal breadth or *J* be then used in an age-year specific equation. Ruff's (2007) distal metaphyseal method is most accurate when used to estimate body mass in children ages 1 to 12 years old. Robbins and colleagues' (2010) *J* method relies on cross-sectional properties of the femur robusticity, that have traditionally been used to estimate activity (Cowgill 2010) and nutritional status (Garn et al. 1964). In juveniles, where the distal epiphyses is unfused, a cross-sectional measure is taken at 45.5% of the total bone length from the distal end, whereas when the distal epiphysis is fused the cross-section is taken at 50% of the total bone length. The method builds on that of O'Neill and Ruff (2004), who used mediolateral and anteroposterior cross-sectional measures to calculate the polar second moment of area, or *J*. *J* acts as an approximation of the total amount of torsional rigidity found in a bone cross-section and can be used to examine loading history.

There are some additional body mass estimation methods that are used by biological anthropologists. While establishing the method using the distal metaphyseal method, Ruff (2007) also developed an equation for estimating body mass based on femoral head breadth for juveniles over the age of 7 years. Robbins-Schug and colleagues (2013) use panel-regression methods to capitalize on the longitudinal nature of the Denver data, producing new methods for the femoral head, distal femoral metaphysis, and *J*. The advantage of the panel regression method is it uses a single age independent equation, so that age does not need to be estimated from dental development prior to selecting a body mass estimation equation. Yapuncich and colleagues (2018) also used panel regression methods to leverage the Harpenden Growth study, devising a body mass estimation equation derived from bi-iliac breadth measures. While the femoral measurement methods can be taken on dry bones or in medical images such as CT scans, the bi-iliac methods would be difficult if not impossible to use in dry bone due to the lack of soft tissue.

Although it has been proposed that body mass estimation could be used in forensic contexts (e.g. Robbins-Schug et al. 2013; Cowgill 2018), the reliability of the methods have not been established. Robbins-Schug et al. (2013) and Cowgill (2018) presented tests of body mass estimation methods on juvenile remains from multiple skeletal collections. Both studies noted a considerable effect of population membership on estimates of body mass, although these samples were not known-weight and therefore cross-population accuracy of the methods was not established. Only Robbins-Schug and colleagues (2013) have tested body mass estimation methods on a sample of known-weight children. The authors used a sample of 36 children who died in Ohio between 1990 and 1991 to test the performance of both panel (Robbins-Schug et al. 2013) and age-structured equations (Ruff 2007; Robbins-Schug et al. 2010) for body mass estimation. Results of this analysis were promising: the study found a mean bias of -0.11kg for panel regression using the distal metaphysis and a mean bias of -2.18kg when using *J*, However, the test relied on a relatively small number of individuals, and more than half of the test sample was aged 2 years and under (20 individuals, or 55% of the sample). Before juvenile body mass estimation methods can be adopted into forensic practice, these methods should be evaluated using larger samples, and particularly including more individuals over the age of 2 years.

In this paper, we test a body mass estimation method for juveniles aged 0 to 12.5 years of age based on panel regression (Robbins-Schug et al. 2013) to explore its potential for use in forensic contexts. From a forensic anthropology perspective, this method is advantageous compared to the age-structured methods because it does not require an age estimate (e.g. Ruff 2007; Robbins et al. 2010). Using an estimated age to select a body mass estimation formula compounds error in the body mass estimate in unquantified ways, which is undesirable given the push to raise evidentiary standards in forensic anthropology (Christensen and Crowder 2009).To test the panel regression models, we use a sample of post mortem CT scans from the Office of the Medical Investigator (OMI), New Mexico, to measure femoral dimensions in children aged 0-12.5 years at death. We test the consistency of body mass estimates using different measures of skeletal robusticity, and separate our analysis according to age groups to evaluate how growth processes affect the reliability of estimates.

Materials and Methods

Post-mortem CT scans taken at autopsy were collected from the Office of the Medical Investigator (OMI) in Albuquerque, New Mexico. These are high resolution scans with a slice thickness of 1mm and 0.5 overlap, which have been reconstructed with settings optimizing bone visualization. Infants were typically scanned in a single scan, while older children and teenagers were scanned in three scans: one for the head and upper body with the arms crossed over the chest, one of the torso with the arms out of the field of view, and the third of the lower extremities. We limited the test sample to those cases where the individual was 12.5 years at death or younger to match the reference sample used by Robbins-Schug et al (2013). We chose not to include individuals whose cause of death implied a history of chronic disease or significant medical support prior to death, as such disease processes might have altered their weight over a relatively short period, which may not be reflected in their skeletal growth. The causes of death excluded included: cancers of all types, congenital malformations except where they are known to be asymptomatic during life, complications of “extreme” prematurity, fetal deaths, and serious genetic and chronic diseases. The manners of death included in the final sample, after applying the further exclusion criteria described below, is described in further detail in the results section.

For each individual, cadaver length and cadaver weight were recorded from measurements taken at autopsy. The weight measurement protocol at the OMI is to record the weight of the individual as he or she was received in the body bag. In the case of small children, the individual is usually re-weighed once undressed. To eliminate cases where weight measurements were potentially inaccurate, we compared the body mass index (BMI) of the child as calculated from height and weight measurements to the CDC reference standards (Kuczmarski et al. 2002) for children above the age of 2 years, and the WHO reference standards (WHO Multicentre Growth Reference Study Group 2006) for children under the age of 2 years, as recommended by the CDC. Individuals whose BMIs were more than 1 BMI unit greater than the 97^{th} percentile, or more than 1 BMI unit less than the 3^{rd} percentile, were excluded. However, because height could also have been misrecorded in some cases, which would influence the calculation of BMI, we re-included children whose weight was below the 97th percentile or over the 3^{rd} percentile for weight for age of their specific reference standard. Then, individuals in the resulting data pool were categorized as obese if they fell above the 95th percentile of BMI for age. This selection procedure means that the sample includes some overweight and obese individuals, but does not include very obese individuals.

The distal metaphyseal breadth of the femur was taken from the left leg, substituting the right when the left was not available. Measurements were taken using an adaptation of the visualization protocol by Spake and colleagues (2020) that draws upon slab maximum intensity (slab MIP) projection. This protocol is advantageous because it does not require the user to segment the bone to be measured – measurement is performed using the typical three plane viewer, with one of the viewers used as the measurement plane and set to slab MIP mode. The viewers are adjusted to mimic an osteometric board measurement of long bones (see Spake et al. 2020 for more details). In this case, the protocol was modified so that the measurement plane mimicked a sliding caliper by aligning it with the long axis of the metaphysis so that the slab MIP projection replicated the plane of the scale of the caliper (its own measurement plane). Slab MIP allows the visualization of both ends of the bones simultaneously even if they do not occur in the same slice, which is ideal for capturing the maximal extent of the curvature of the medial and lateral portions of the metaphysis (Figure 1).

Polar moment of inertia (*J*) measurements were also taken from the left leg, substituting the right when the left was not available. Orientation of the bones and measurements were, again, conducted using the protocol by Spake and colleagues (2020). Femurs were oriented to mimic positioning on an osteometric board so the full length of the diaphysis could be measured. As the sample consisted of individuals with unfused, and partially fused proximal and distal epiphyses the decision was made to measure the total length of the diaphysis, instead of the total bone length, in order to maintain a consistent methodology across the sample. As such diaphyseal length was determined by measuring the distance between the most distal portion of the distal metaphysis and the most proximal portion of the proximal metaphysis. Fusion lines were still visible in older individuals in the sample, making it possible to determine the end point of the metaphysis. Since the diaphysis was used, cross-sections of the midpoint were taken at 45.5% of the diaphyseal length (beginning from the distal end). The 45.5% measurement best corresponds to the location of the 50% midpoint in femurs with fused distal epiphyses due to said epiphysis's larger contribution to biomechanical length (Ruff 2003). At the midpoint cross-section, measurements of the total maximum mediolateral (ML) and anteroposterior (AP) bone width were taken (Figure 2a), as well as measures of the maximum mediolateral (ml) and anteroposterior (ap) width of the medullary cavity were taken from the transverse cross-section (Figure 2b). All measurements were taken in millimetres. *J* was then calculated from these measures in accordance with the formula laid out by O'Neill and Ruff (2004), in order to replicate the method used by Robbins-Schug and colleagues (2013).

Body mass was estimated from these two measurements using the formulae presented by Robbins-Schug and colleagues (2013). To respect the limits of the equations, we removed individuals whose measurements for the predictor variables fell out of the ranges for the Denver sample, which was the reference sample for the method. These ranges are available in the supplementary material of the original paper and were 25.3 to 68.6 mm for the breadth of the distal metaphysis of the femur and 413 to 32811 mm^4 for *J* (Robbins-Schug et al. 2013).

For each of the two body mass estimation formulae, the residual was calculated as the estimate minus the real weight, meaning that a negative residual indicates underestimation and a positive residual indicates overestimation. To explore the performance of the formulae, the mean residual (MR) and mean absolute residual (MAR) were calculated as measures of accuracy and precision respectively. The MR was then compared against zero with a one sample t-test. These measures were calculated for the sample as a whole, and then repeated for the sample broke down into age groups based on a modified version of life history stages as follows: infant (0-3 years); child (3-7 years); juvenile (7-12.5 years). These age groups were adapted from the life history stages as proposed by Bogin (1999). This scheme defines the beginning of adolescence at 10 years for females and 12 years for males. However, due to the truncation of the test sample at 12.5 years to match the reference sample used by Robbins-Schug et al. (2013), an adolescent category would have included few individuals and been composed predominantly of girls. Thus, we opted to collapse the adolescent life history stage into the juvenile stage. The method did not include information to calculate a 95% prediction interval, and therefore we can only report the accuracy of the point estimates.

Results

The final test sample after all exclusions included 94 individuals (42 females and 52 males). These individuals died primarily of accidents (n = 52 or 55%), a very small number died of suicide (n = 3 or 3%), and the remainder of individuals were roughly evenly split between natural deaths (n = 17 or 18%) and deaths by homicide (n = 22 or 23%). A breakdown of the sample by age and sex is available in Figure 3. Of these individuals, 20 were considered obese (above the 95th percentile of BMI for age), yielding an obesity rate for all children in the sample of 21.3%. This is consistent with New Mexico child obesity rates, which are reported at 13.9% for kindergarteners and 19.9% for third graders (New Mexico Department of Health 2017). New Mexico's child obesity rates are consistent with or slightly higher than current US rates of 13.9% for children 2-5 years and 18.4% for children 6-11 years of age (Hales et al. 2017). The distribution of BMI in the children included in this study by age group and sex is available in Figure 4 and in Table 1.

Mean residual (MR) and mean absolute residual (MAR) for each of the body mass estimation formulae, for the whole sample as well as each age category are available in Table 2. The formula using the breadth of the distal metaphysis generally underestimated weight in the entire sample by an average of 2.23kg (the overall MR). However, this difference was not uniform. In the youngest individuals (infant category), the formula actually had a positive bias, and overestimated weight by 0.92kg. With progressing age, the formula increasingly underestimated weight so that in the juvenile age group, the formula underestimated weight by an average of 8.72kg. The precision of the metaphyseal method decreased with age as indicated by an increasing MAR, which is consistent with the heteroscedastic nature of growth.

Similar trends were observed for the formula using *J*, however, this formula underestimated weight less than the one using the breadth of the distal metaphysis. In the overall sample, the formula using *J* underestimated weight by an average of 1.24kg. Again, in the youngest individuals (infant age group) weight was overestimated by 1.10kg, and in the juvenile age groups weight was underestimated by an average of 4.76kg. Here again, precision decreased with increasing age. Although the MAR for the *J* formula was slightly larger in the younger age groups than it was for the metaphyseal formula, the *J* formula had a much smaller MAR than the metaphyseal formula in the oldest age group. This indicates that the precision of the *J* formula is less affected by age than that of the metaphyseal formula. A visual comparison of real body weight versus body weight estimated by the breadth of the metaphysis and by *J* is available in Figure 5, and confirms that while both methods underestimate body weight, the formula based on *J* yields more accurate estimates of body weight.

Discussion

Results from this test of the Robbins-Schug et al. (2013) body mass estimation methods are not promising. Both the formula using the breadth of the distal metaphysis and the one using *J* showed significant error and bias at nearly all ages. Body mass was underestimated at most ages, and this error increased with age so that older children's weights were markedly underestimated. This is consistent with findings from another test by Yim and colleages (2020), which tested the age-specific *J* formulae presented by Robbins et al. (2010) against the panel regression *J* formula by Robbins-Schug et al. (2013), which was also tested here. Yim and colleagues found that both the age-specific and the panel regression formulae underestimated weight, but that the underestimation was more marked for the panel-regression formula.

Of the two methods tested in this study, the formula using *J* performed better than the formula using the breadth of the distal metaphysis. Interestingly, the authors of the original paper recommended that that the panel regression model based on metaphyseal breadth should be preferred as it seemed to perform better in testing (Robbins-Schug et al. 2013). Cowgill (2018) found *J* to yield higher estimates of body mass than metaphyseal breadth, although her sample was archaeological and did not allow for quantification of the accuracy of the methods. Cowgill's study may also have produced higher *J*-based estimates due to the increased levels of activity found in her sample populations compared to those occurring in the reference population for the formulae (the Denver Growth Study). The OMI sample used in this study and the Denver Growth Study are both comprised of individuals from contemporary American populations, meaning they had access to (relatively) modern medical care and would be noticeably more sedentary than most archaeological populations (Ruff et al. 1993, Ruff 2005). The outcome of the lower activity level in modern populations would likely produce lower *J* values, a trend that has been noted in adults (Pearson 2000, Stock 2006). It should be noted that even within the temporal space between the collection of the 20th century Denver Growth Study and the 21st century OMI sample, there has been a marked reduction in activity in the US, especially in children (Manson et al. 2004). *J* is thought to reflect changes in body mass more accurately than metaphyseal measures as it increases due to strengthening of the bone in direct response to the increased loading and increased mass that occur throughout growth (Pomeroy et al. 2018, Swan et al. 2020). This may make *J* a better candidate for body mass estimation because it is a measure with more plasticity in response to body mass, relative to metaphyseal dimensions that may be more canalized because of the demands of locomotion (Cowgill et al. 2010). Indeed, in our sample *J* performs better for estimation of mass except in infants, an age category where many children have not walked regularly and therefore have not loaded the bones consistently. However, while it has been demonstrated that cross-sectional properties of long bones act as reliable predictors of lean mass, cross-sectional properties have been shown to be less reliable predictors of fat mass in both children and adults (Petit et al. 2005, Pomeroy et al. 2018). As Robbins-Schug and coworkers (2013) found, in our sample the log of weight was more tightly correlated to the log of *J* (R = 0.96) than the log of weight was to the log of the breadth of the distal metaphysis of the femur (R = 0.92).

The dramatically increasing error with age was somewhat unexpected (see Figure 6), in that the residuals exhibited an exponential pattern when visually examined. Although growth is heteroscedastic and variation is known to increase with age, this should be reflected in greater residual variance around zero, or with some directional bias when reference and target samples do not share population growth trajectories, rather than the exponential increase in error noted here. In model development, a non-random pattern in residuals such as exponential patterning typically suggests that an alternative model which fits the data more closely should be sought (Martin et al. 2017). While Robbins-Schug et al. (2013) did not present a plot of residuals, or of estimated versus real body mass from which residual patterning could be inferred, other tests of these panel regression models have found similar patterning of residuals. Yim et al. (2020) tested the age-structured regression (Robbins et al. 2010) and the panel regression (Robbins- Schug et al. 2013) formulae based on *J*. Their results suggested a pattern of residuals for the panel regression formulae similar to the ones reported here. However, the nearly exponential relationship was not present for age-structured equations.

In our analysis, this increasing bias with age cannot be convincingly attributed to the additional weight of personal belongings such as clothing which were included in the weight of some of the OMI individuals. One study found that clothing weights on average 0.8-1.12 kg (Wigham et al. 2013), and even if this value is doubled or even tripled to account for the presence of shoes and outerwear, it does not reach the average residual for juveniles of 8.72kg for the breadth of the distal metaphysis of the femur, although it begins to approach that of 4.76kg for juveniles using *J*. Rather, this pattern of residuals might stem from the original modeling procedure, wherein both the predictor and dependent variables were logged prior to fitting with linear regression. Detransformation bias is a known problem with logged dependent variables, which results from the fact that the correct de-transformed estimate is not obtained by exponentiating the output of the linear regression (Smith 1993, Feng et al. 2013). Others performing log transformation for juvenile body mass estimation have provided correction factors (Ruff 2007). The exponentiated result should be expected to be less than the correct estimate as they represent the geometric and arithmetic means respectively (Smith 1993). Indeed, when Robbins-Schug and colleagues (2013, Table 4) compare the difference between their exponentiated predictions, which they term the median, and the median of previously calculated age-specific regression, the exponentiated predictions are smaller than the medians of the age-specific regression equations. The bias, as they term it, is greater for the formula using breadth of the distal metaphysis than it is for the formula using *J*. This effect is mirrored in our results and illustrated in Figure 6, wherein residuals are plotted against age.

While potentially important, the choice of log transformation for modelling the relationship between femoral dimensions and weight is likely only one reason for the frequency of weight underestimation. Another factor likely contributing to this bias is the secular trends occurring between when the Denver Growth Study was conducted and today. The Robbins-Schug et al. (2013) equations are based on data from the Denver Growth Study, as are the equations from Ruff (2007) and Robbins et al. (2010). Indeed, when tested on children with higher BMI living in the 1990s in Ohio, the models based on the Denver population underestimated weight (Robbins et al. 2010). While some argue that body mass estimation methods should less affected by inter-population error than other estimation methods for other aspects of the biological profile because it is based on allometric relationships (Ruff 2007; Yim et al. 2020), others have recognized that a body mass estimation method based on a "modern" sample such as the Denver Growth Study may not be adequate for use in paleoanthropology where Late Pleistocene individuals are concerned (Cowgill et al. 2018). It is important to acknowledge that this works both ways: the Denver Growth study may not be adequate for past populations, but it is not necessarily adequate for contemporary ones either.

Denver Growth study operated between the 1920s and 1960s. At the time, enrolled subjects were noted to be of higher socioeconomic status relative to the Denver area, and to be larger and heavier than children enrolled in other contemporary growth studies in the US (Maresh 1970; Maresh and Beal 1970). However, since this time the US has experienced secular trends in growth, particularly manifesting in greater weight and BMI for age (Sun et al. 2012; Vijayakumar et al. 2018), and to a lesser extent increased height for age (Bock and Sykes 1989; Freedman et al. 2000; Vijayakumar et al. 2018; but see also Komlos and Lauderdale 2007). Indeed, testing of the panel regression methods on a sample from Ohio dating to the 1990s found that the method underestimated mass (Robbins-Schug et al. 2013), in agreement with our results. In describing his analysis of the same sample of children from the Denver Growth Study as used by Robbins-Schug and colleagues, Ruff (2007) indicates that two outliers were present in his data, and in both cases, these individuals fell above the 95th percentile for BMI for age (cut-off point for classifying obesity). While Ruff does not provide descriptive statistics for weight, or the rate of either overweight or obesity in his sample, he states that the two outlying individuals (BMI over 95th percentile) were removed. It is therefore reasonable to assume that the sample used to derive this group of body mass estimation methods includes few overweight and perhaps no obese individuals at all. In contrast, 21.2% of our test sample fell into the obese range as defined by falling above the 95th centile for BMI for age. When this lack of representation of obese individuals in the Denver Growth Study, combined with the increase in both diversity and obesity in US children since the early to mid-19th century (Mehta et al. 2013, Burwell et al. 2016), body mass estimation on contemporary children performed with methods based on the Denver Growth Study (Ruff 2007; Robbins et al. 2010; Robbins-Schug et al. 2013) are likely to yield biased or even inaccurate results.

Weight-based exclusion criteria were used to exclude cases with potential data entry errors, as well as to parse out individuals where weights may have included medical implements or clothing. In addition, we excluded individuals whose measured metaphyseal breadth or *J* value fell outside the range of measurements included in the reference sample used by Robbins-Schug and colleagues (2013). However, forensic anthropology cases may include disproportionate numbers of individuals from a low socioeconomic background, or who have experienced histories of neglect and/or abuse (Spake and Cardoso 2018; Spake et al. n.d.). In the U.S., individuals from a low socioeconomic status groups have higher rates of obesity (Rogers et al. 2015), and those with histories of abuse and/or neglect may be exceptionally short and thin for age (see Table 1 in Spake and Cardoso 2018, as well as references cited therein). Thus, it is possible that the exclusion criteria applied in this study may have excluded the individuals who would be more likely to be the subjects of forensic anthropological evaluation. In developing body mass estimation methods, a key consideration is the range of variation in weight for age included in the reference sample, just as adequate variation in growth status for age must be considered when developing juvenile age estimation methods.

Some have proposed that because body mass estimation is based on an allometric relationship between body size and bone size, its accuracy should be less relatively independent from population variation (Yim et al. 2020). However, the results of this study as well as analyses by Robins-Schug et al. (2010) and Cowgill (2018) suggest that this is not the case. Body mass estimation appears to be sensitive to variation in body composition, which is due to a mixture of environmental factors including nutritional and socioeconomic conditions. Elsewhere, we have explored the concept of growth-appropriate methods (Spake et al. 2021.; Cardoso et al. 2021) as an alternative to population-specific methods. The idea of a population-specific method carries the implication that in order to perform well on a target sample, a method must be based on a reference sample that is biologically similar, i.e., that shares the same ancestry. However, we have shown that for age estimation, which is based on growth, methods perform best when the reference and target samples are matched based on the basis of shared ontogenic environment rather than presumed ancestry (Cardoso et al. 2021). A similar rationale can be applied to juvenile body mass estimation, as body composition does change across the growth trajectory (Wells 2006). Thus, we suggest that body mass estimation methods should also be growth-appropriate, in that a method should be selected based on matching the aspects of ontogenic environments which influence body composition, rather than matching based on presumed ancestry. This is supported by the results of this analysis which suggests that although the reference sample was derived from individuals with similar presumed ancestry to that of the target sample, differences in ontogenic environment caused weight to be systematically underestimated in the target sample.

Clearly, lesser-explored aspects of the juvenile biological profile are not free of the problems which affect juvenile age estimation methods. This is a logical conclusion because body mass estimation in juveniles inherently has to account for growth-related changes in dimensions of the skeleton, as is true for age estimation and any other aspect of the biological profile in juveniles. This means that attempts to explore skeletal estimation methods in juveniles should be carefully considered and draw from the lessons learned by the juvenile age estimation literature. Key discussions in the juvenile age estimation literature include appropriate statistical modelling of growth, which is in its nature a complex non-linear and heteroscedastic process, population-based variation in traits and understanding their underlying causes, and selecting estimation methods based on growth-appropriateness.

Perspectives

Body mass estimation may eventually become useful in forensic investigations as an additional piece of the biological profile, but as of now available methods are not appropriate for forensic use. Although the wider adoption of medical imaging has produced an unprecedented wealth of data on the juvenile skeleton, it is important to keep an anthropological lens when analyzing the data. As others are recognizing for other traits of the biological profile, it is not enough to use data to produce models and methods; we must also seek to understand the biological processes that produce the data or we risk creating misleading methods that potentially impede identifications (DiGangi and Bethard, 2021). Results from this study reinforce the importance of continuing to probe the underlying reasons for population variation in order to develop better skeletal estimation methods. Both intra and inter population variation remain key obstacles in method transportability in forensic anthropology. Leveraging medical imaging to increase availability of skeletal data from around the world stemming from medical imaging, should help to better understand the underlying causes of this variation.

Acknowledgments

We thank Briana New and Bridget Algee-Hewitt for the invitation to contribute to this Special Issue. This study stems from a project funded by Mitacs Canada (IT13950), NSERC (RGPIN-201-05863) and the Department of Archaeology at Simon Fraser University. During the writing of this manuscript, LS was supported by the John Templeton Foundation.

Received 9 October 2020; accepted for publication 1 June 2021.

Literature Cited

Alemán, I., J. Irurita, A. R. Valencia et al. 2012. Brief communication: The Granada osteological collection of identified infants and young children. *Am. J. Phys. Anthropol.* 149:606–610.

Belcastro, M. G., B. Bonfiglioli, M. E. Pedrosi et al. 2017. The history and composition of the identified human skeletal collection of the Certosa Cemetery (Bologna, Italy, 19th–20th century). *Int. J. Osteoarchaeol.* 27:912–925.

Black, T. K. 1978. Sexual dimorphism in the tooth-crown diameters of the deciduous teeth. *Am. J. Phys. Anthropol.* 48:77–82.

Bock, R. D., and R. C. Sykes. 1989. Evidence for continuing secular increase in height within families in the United States. *Am. J. Hum. Biol.* 1:143–148.

Buck, T. J., and U. Strand Vidarsdóttir. 2004. A proposed method for the identification of race in sub-adult skeletons: A geometric morphometric analysis of mandibular morphology. *J. Forensic Sci.* 49:1–6.

Burwell, S., J. Philpott, J. N. and Robles. 2016. United to reduce childhood obesity in North America. *Rev. Panam. Salud Publica* 40:78–79.

Cardoso, H. F. V. 2006. The collection of identified human skeletons housed at the Bocage Museum (National Museum of Natural History) in Lisbon, Portugal. *Am. J. Phys. Anthropol.* 129:173–176.

Cardoso, H. F. V. 2008. Sample-specific (universal) metric approaches for determining the sex of immature human skeletal remains using permanent tooth dimensions. *J. Archaeol. Sci.* 35:158–168.

Cardoso, H. F. V. 2010. Testing discriminate functions for sex determination from deciduous teeth. *J. Forensic Sci.* 55:1,557–1,560.

Cardoso, H. F. V., and S. R. Saunders. 2008. Two arch criteria of the ilium for sex determination of immature skeletal remains: A test of their accuracy and an assessment of intra- and inter-observer error. *Forensic Sci. Int.* 178:24–29.

Cardoso, H. F. V., L. Spake, L. Ríos et al. 2021. Population variation in diaphyseal growth and age estimation of juvenile skeletal remains. In *Remodeling Skeletal Age: Modern Applications and New Research Directions*, B. F.B. Algee-Hewitt and K. Jieun, eds. London: Academic Press, 99–138.

Cattaneo, C., D. Mazzarelli, A. Cappella et al. 2018. A modern documented Italian identified skeletal collection of 2127 skeletons: The CAL Milano Cemetery Skeletal Collection. *Forensic Sci. Int.* 287:219.e1–219.e5.

Christensen, A. M., and C. M. Crowder. 2009. Evidentiary standards for forensic anthropology. *J. Forensic Sci.* 54:1,211–1,216.

Cowgill, L. W. 2018. Juvenile body mass estimation: A methodological evaluation. *J. Hum. Evol.* 115:78–84.

Cowgill, L. W., A. Warrener, H. Pontzer et al. 2010. Waddling and toddling: The biomechanical effects of an immature gait. *Am. J. Phys. Anthropol.* 143:52–61.

De Vito, C., and S. R. Saunders. 1990. A discriminant function analysis of deciduous teeth to determine sex. *J. Forensic Sci*. 35:845–858.

DiGangi, E. A., and J. D. Bethard. 2021. Uncloaking a lost cause: Decolonizing ancestry estimation in the United States. *Am. J. Phys. Anthropol.* 175:422–436.

Fan, F., K. Zhang, Z. Peng et al. 2016. Forensic age estimation of living persons from the knee: Comparison of MRI with radiographs. *Forensic Sci. Int.* 268:145–150.

Feldesman, M. R. 1992. Femur/stature ratio and estimates of stature in children. *Am. J. Phys. Anthropol.* 87:447–459.

Feng, C., H. Wang, N. Lu et al. 2013. Log transformation: Application and interpretation in biomedical research. *Stat. Med.* 32:230–239.

Freedman, D. S., L. K. Khan, M. K. Serdula et al. 2000. Secular trends in height among children during 2 decades: The Bogalusa Heart Study. *Arch. Pediatr. Adolesc. Med.* 154:155–161.

Garn, S. M., C. G. Rohmann, M. Béhar et al. 1964. Compact bone deficiency in protein-calorie malnutrition. *Science* 145:1,444–1,445.

Grabherr, S., C. Cooper, S. Ulrich-Bochsler et al. 2009. Estimation of sex and age of "virtual skeletons": A feasibility study. *Eur. Radiol.* 19:419–429.

Hales, C. M., M. D. Carroll, C. D. Fryar et al. 2017. *Prevalence of Obesity Among Adults and Youth: United States, 2015–2016.* NCHS Data Brief No. 288, October 2017. Centers for Disease Control and Prevention. https://www.cdc.gov/nchs/products/databriefs/db288.htm.

Hassett, B. 2011. Estimating sex using cervical canine odontometrics: A test using a known sample. *Am. J. Phys. Anthropol.* 146:483–489.

Komlos, J., and B. E. Lauderdale. 2007. The mysterious trend in American heights in the 20th century. *Ann. Hum. Biol.* 34:206–215.

Kuczmarski, R. J., C. L. Ogden, S. S. Guo et al. 2002. 2000 CDC Growth charts for the United States: Methods and development. *Vital Health Stat. 11* 11:1–190.

Macaluso, P. J. 2011. Investigation on the utility of permanent maxillary molar cusp areas for sex estimation. *Forensic Sci. Med. Pathol.* 7:233–247.

Manson, J. E., P. J. Skerrett, P. Greenland et al. 2004. The escalating pandemics of obesity and sedentary lifestyle: A call to action for clinicians. *Arch. Intern. Med.* 164:249–258.

Maresh, M. M. 1970. Measurements from roentgenograms. In *Human Growth and Development*, R. W. McCannon, ed. Springfield, IL: C. C. Thomas, 157–188.

Maresh, M. M., and V. A. Beal. 1970. A longitudinal survey of nutrition intake, body size, and tissue measurements in healthy subjects during growth. *Monogr. Soc. Res. Child Dev.* 35:33–39.

Martin, J., D. D. R. de Adana, and A. G. Asuero. 2017. Fitting models to data: Residual analysis, a primer. In *Uncertainty Quantification and Model Calibration*, J. P. Hessling, ed. Rijeka, HR: Intech, 133–174.

Mehta, N. K., L. Hedwig, and K. R. Ylitalo. 2013. Child health in the United States: Recent trends in racial/ethnic disparities. *Soc. Sci. Med.* 95:6–15.

Mittler, D., and S. Sheridan. 1992. Sex determination in subadults using auricular surface morphology: A forensic science perspective. *J. Forensic Sci.* 37:1,068–1,075.

Molleson, T., and K. Cruse. 1998. Some sexually dimorphic features of the human juvenile skull and their value in sex determination in immature skeletal remains. *J. Archaeol. Sci.* 25:719–728.

New Mexico Department of Health. 2018. *The Weight of Our Children: New Mexico Childhood Obesity 2017 Update.* Santa Fe, NM: New Mexico Department of Health. https://www.nmhealth.org/data/view/chronic/2113/.

O'Donnell, A., S. D. Berry, and H. J. H. Edgar. 2017. Can cephalometrics discriminate between the sexes in a diverse juvenile sample? *J. Forensic Sci.* 62:735–740.

O'Neill, M. C., and C. B. Ruff. 2004. Estimating human long bone cross-sectional geometric properties: A comparison of noninvasive methods. *J. Hum. Evol.* 47:221–235.

Pearson, O. M. 2000. Activity, climate, and postcranial robusticity: Implications for modern human origins and scenarios of adaptive change. *Curr. Anthropol.* 41:569–607.

Petit, M. A., T. J. Beck, J. Shults et al. 2005. Proximal femur bone geometry is appropriately adapted to lean mass in overweight children and adolescents. *Bone* 36:568–576.

Pomeroy, E., A. Macintosh, J. C. K. Wells et al. 2018. Relationship between body mass, lean mass, fat mass, and limb bone cross-sectional geometry: Implications for estimating body mass and physique from the skeleton. *Am. J. Phys. Anthropol.* 166:56–69.

Robbins, G., P. W. Sciulli, and S. H. Blatt. 2010. Estimating body mass in subadult human skeletons. *Am. J. Phys. Anthropol.* 143:146–150.

Robbins-Schug, G., S. Gupta, L. W. Cowgill et al. 2013. Panel regression formulas for estimating stature and body mass from immature human skeletons: A statistical approach without reference to specific age estimates. *J. Archaeol. Sci.* 40:3,076–3,086.

Rogers, R., T. F. Eagle, A. Sheetz et al. 2015. The relationship between childhood obesity, low socioeconomic status, and race/ethnicity: Lessons from Massachusetts. *Child. Obes.* 11:691–695.

Ruff, C. 2003. Growth in bone strength, body size, and muscle size in a juvenile longitudinal sample. *Bone* 33:317–329.

Ruff, C. B. 2005. Mechanical determinants of bone form: Insights from skeletal remains. *J. Musculoskelet. Neuronal Interact.* 5:202–212.

Ruff, C. 2007. Body size prediction from juvenile skeletal remains. *Am. J. Phys. Anthropol.* 716:698–716.

Ruff, C. B., and M. Niskanen. 2018. Introduction to special issue: Body mass estimation — Methodological issues and fossil applications. *J. Hum. Evol.* 115:1–7.

Ruff, C. B., E. Trinkaus, A. Walker et al. 1993. Postcranial robusticity in *Homo*. I: Temporal trends and mechanical interpretation. *Am. J. Phys. Anthropol.* 91:21–53.

Scheuer, L. 2002. A blind test of mandibular morphology for sexing mandibles in the first few years of life. *Am. J. Phys. Anthropol.* 119:189–191.

Schmidt, S., M. Mühler, A. Schmeling et al. 2007. Magnetic resonance imaging of the clavicular ossification. *Int. J. Legal Med.* 121:321–324.

Schutkowski, H. 1993. Sex determination of infant and juvenile skeletons: I. Morphognostic features. *Am. J. Phys. Anthropol*. 90:199–205.

Serin, J., C. Rérolle, J. Pucheux et al. 2016. Contribution of magnetic resonance imaging of the wrist and hand to forensic age assessment. *Int. J. Legal Med.* 130:1,121–1,128.

Smith, R. J. 1993. Logarithmic transformation bias in allometry. *Am. J. Phys. Anthropol.* 90:215–228.

Smith, S. L. 2007. Stature estimation of 3–10-year-old children from long bone lengths. *J. Forensic Sci.* 52:538–546.

Spake, L., S. Blau, and H. F. V. Cardoso. 2021. The impact of forensic mortality bias in juvenile age estimation. *Eur. J. Anat.* 25:129–146.

Spake, L., and H. F. V. Cardoso. 2018. Are we using the appropriate reference samples to develop juvenile age estimation methods based on bone size? An exploration of growth differences between average children and those who become victims of homicide. *Forensic Sci. Int.* 282:1–12.

Spake, L., J. Meyers, S. Blau et al. 2020. A simple and software-independent protocol for the measurement of post-cranial bones in anthropological contexts using thin slab maximum intensity projection. *Forensic Imaging* 20:200354.

Stock, J. T. 2006. Hunter-gatherer postcranial robusticity relative to patterns of mobility, climatic adaptation, and selection for tissue economy. *Am. J. Phys. Anthropol.* 131:194–204.

Stull, K. E., E. N. L’Abbé, and S. D. Ousley. 2014. Using multivariate adaptive regression splines to estimate subadult age from diaphyseal dimensions. *Am. J. Phys. Anthropol.* 154:376–386.

Stull, K. E., E. N. L’Abbé, and S. D. Ousley. 2017. Subadult sex estimation from diaphyseal dimensions. *Am. J. Phys. Anthropol.* 163:64–74.

Sun, S. S., X. Deng, R. Sabo et al. 2012. Secular trends in body composition for children and young adults: The Fels Longitudinal Study. *Am. J. Hum. Biol.* 24:506–514.

Sutter, R. C. 2003. Nonmetric subadult skeletal sexing traits: I. A blind test of the accuracy of eight previously proposed methods using prehistoric known-sex mummies from northern Chile. *J. Forensic Sci.* 48:927–935.

Swan, K. R., R. Ives, L. A. B. Wilson et al. 2020. Ontogenetic changes in femoral cross-sectional geometry during childhood locomotor development. *Am. J. Phys. Anthropol.* 173:80–95.

Telkk, A., A. Palkama, and P. Virtama. 1962. Prediction of stature from radiographs of long bones in children. *J. Forensic Sci.* 7:474–479.

Teschler-Nicola, M., and H. Prossinger. 1998. Sex determination using tooth dimensions. In *Dental Anthropology: Fundamentals, Limits, and Prospects*, K. W. Alt, F. W. Rösing, and M. Teschler-Nicola, eds. Vienna, AT: Springer, 479–500.

Viciano, J., I. Alemán, R. D'Anastasio et al. 2011. Odontometric sex discrimination in the Herculaneum sample (79 AD, Naples, Italy), with application to juveniles. *Am. J. Phys. Anthropol.* 145:97–106.

Viciano, J., S. López-Lázaro, and I. Alemán. 2013. Sex estimation based on deciduous and permanent dentition in a contemporary Spanish population. *Am. J. Phys. Anthropol.* 152:31–43.

Viciano, J., C. Tanga, R. D'Anastasio et al. 2020. Sex estimation by odontometrics of nonadult human remains from a contemporary Italian sample. *Am. J. Phys. Anthropol.* 175:59–80.

Vijayakumar, P., K. M. Wheelock, S. Kobes et al. 2018. Secular changes in physical growth and obesity among southwestern American Indian children over four decades. *Pediatr. Obes.* 13:94–102.

Vlak, D., M. Roksandic, and M. A. Schillaci. 2008. Greater sciatic notch as a sex indicator in juveniles. *Am. J. Phys. Anthropol.* 137:309–315.

Weaver, D. S. 1980. Sex differences in the ilia of a known sex and age sample of fetal and infant skeletons. *Am. J. Phys. Anthropol.* 52:191–195.

Wells, J. C. K. 2006. The evolution of human fatness and susceptibility to obesity: An ethological approach. *Biol. Rev. Camb. Philos. Soc.* 81:183–205.

WHO Multicentre Growth Reference Study Group. 2006. *WHO Child Growth Standards: Length/Height-for-Age, Weight-for-Age, Weight-for-Length, Weight-for-Height and Body Mass Index-for-Age: Methods and Development*. Geneva, CH: World Health Organization.

Wigham, L. D., D. A. Schoeller, L. K. Johnson et al. 2013. Effect of clothing weight on body weight. *Int. J. Obes. (Lond.)* 37:160–161.

Wilson, L. A. B., H. F. V. Cardoso, and L. T. Humphrey. 2011. On the reliability of a geometric morphometric approach to sex determination: A blind test of sex criteria of the juvenile ilium. *Forensic Sci. Int.* 20:35–42.

Wilson, L. A., N. MacLeod, and L. T. Humphrey. 2008. Morphometric criteria for sexing juvenile human skeletons using the ilium. *J. Forensic Sci.* 53:269–278.

Yapuncich, G. S., S. E. Churchill, N. Cameron et al. 2018. Morphometric panel regression equations for predicting body mass in immature humans. *Am. J. Phys. Anthropol.* 166:179–195.

Yim, A. D., L. W. Koningsberg, H. L. Hwa et al. 2020. Subadult body mass estimation from skeletal remains: Validation for femoral cross-section methods in a contemporary Taiwanese population. In *Program of the Annual Meeting of the American Academy of Forensic Sciences, February 2020, Anaheim, CA, USA.* Colorado Springs, CO: AAFS, 116.

Żądińska, E., M. Karasińska, K. Jedrychowska-Dańska et al. 2008. Sex diagnosis of subadult specimens from Medieval Polish archaeological sites: Metric analysis of deciduous dentition. *Homo.* 59:175–187.

Table 1. Number of Individuals, Mean and Range of Weight, Mean and Range of BMI, and Number and Percentage of Overweight Individuals for Each Age Category, for the Sexes Separately and Combined

Descriptive statistics are given after all exclusions have been applied.

	N	Mean weight (range)	Mean BMI (range)	Number overweight (%)
Total sample				
Females	42	23.15 (4.04-60.00)	17.79 (11.41-26.58)	9 (21.4%)
Males	52	18.61 (5.62-53.00)	16.99 (11.46-24.47)	11 (21.1%)
Sexes combined	94	20.64 (4.04-60.00)	17.35 (11.41-26.58)	20 (21.3%)
Infant				
Females	18	9.99 (4.04-14.40)	15.94 (11.41-18.95)	1 (5.0%)
Males	24	11.30 (5.62-18.4)	16.82 (13.79-24.47)	4 (16.7%)
Sexes combined	42	10.74 (4.04-18.4)	16.44 (11.41-24.47)	5 (11.9%)
Child				
Females	9	19.72 (13.20-31.40)	17.14 (12.78-23.74)	3 (33.3%)
Males	16	18.8 (11.97-27.00)	17.05 (11.97-23.49)	6 (37.5%)
Sexes combined	25	19.15 (11.97-31.4)	17.09 (11.97-23.74)	9 (36.0%)
Juvenile				
Females	15	40.98 (26.40-60.00)	20.39 (16.66-25.58)	5 (33.3%)
Males	12	32.92 (21.20-53.00)	17.23 (11.46-22.64)	1 (8.3%)
Sexes combined	27	37.40 (21.20-60.00)	18.98 (11.46-26.56)	6 (22.2)

Table 2. Residual Analysis for the Formulae Using the Breadth of the Distal Femoral Metaphysis and *J*

For each formula, the number of individuals (N), the range of weights of individuals in the category (Range), mean residual (MR) and mean absolute residual (MAR) are given for the total sample and for the age groups individually. Range, MR and MAR are expressed in kg.

	Breadth of the distal femoral metaphysis	*J*
Total sample		
N	90	88
Range	4.04-60.00	4.04-59.80
MR	-2.23**	-1.24**
MAR	3.96	3.01
Infants		
N	41	40
Range	4.04-18.40	4.04-15.40
MR	0.92**	1.10**
MAR	1.52	1.66
Child		
N	25	24
Range	12.00-31.40	12.00-31.40
MR	-1.18	-1.62*
MAR	2.94	3.06
Juvenile		
N	24	24

Range	21.20-60.00	22.70-59.80
MR	-8.72**	-4.76**
MAR	9.20	5.20

* Mean residual is significantly different from zero at the $p < 0.05$ level

** Mean residual is significantly different from zero at the $p < 0.01$ level

Figure Captions

Figure 1. Measurement of the width of the distal metaphysis of the femur using slab MIP visualization.

Figure 2. A) Mediolateral and anteroposterior measurements of the total cross-section taken at the midpoint (45.5%) of the femoral diaphysis. B) Mediolateral and anteroposterior measurements of the medullary cross-section taken at the midpoint (45.5%) of the femoral diaphysis. In both, the blue line represents the anteroposterior axis and the pink line represents the mediolateral axis.

Figure 3. Composition of the test sample, by sex and age.

Figure 4. Boxplots of the median and quartiles of body mass index (BMI) for females and males, for each age group separately.

Figure 5. Comparison of the performance of the two body mass estimation formula. Real weight is plotted against (A) the body weight estimates yielded by the distal metaphysis; (B) the body weight estimate yielded by *J*. A loess smooth (solid line) is fit to illustrate the relationship between the real and estimated weight, and a dotted line denotes a perfect relationship.

Figure 6. Residual of a) body weight estimated from the breadth of the distal metaphysis and b) *J* over the age range included in the test sample. Negative residuals indicate that weight was underestimated.

Figure 1.

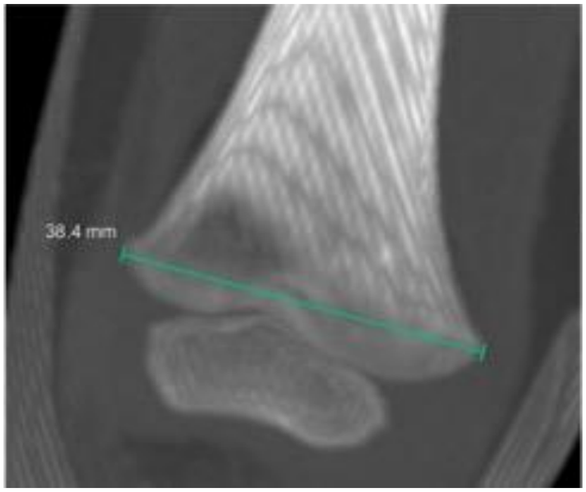

Figure 2.

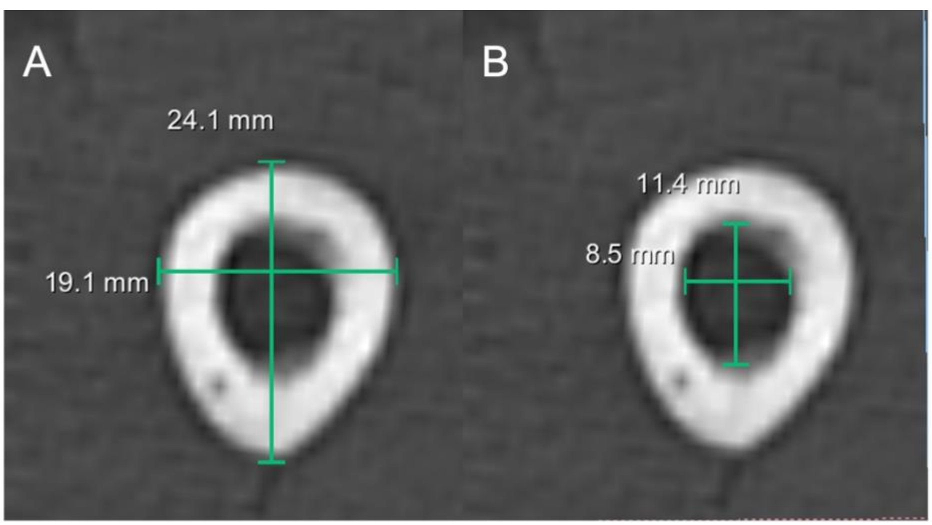

Figure 3.

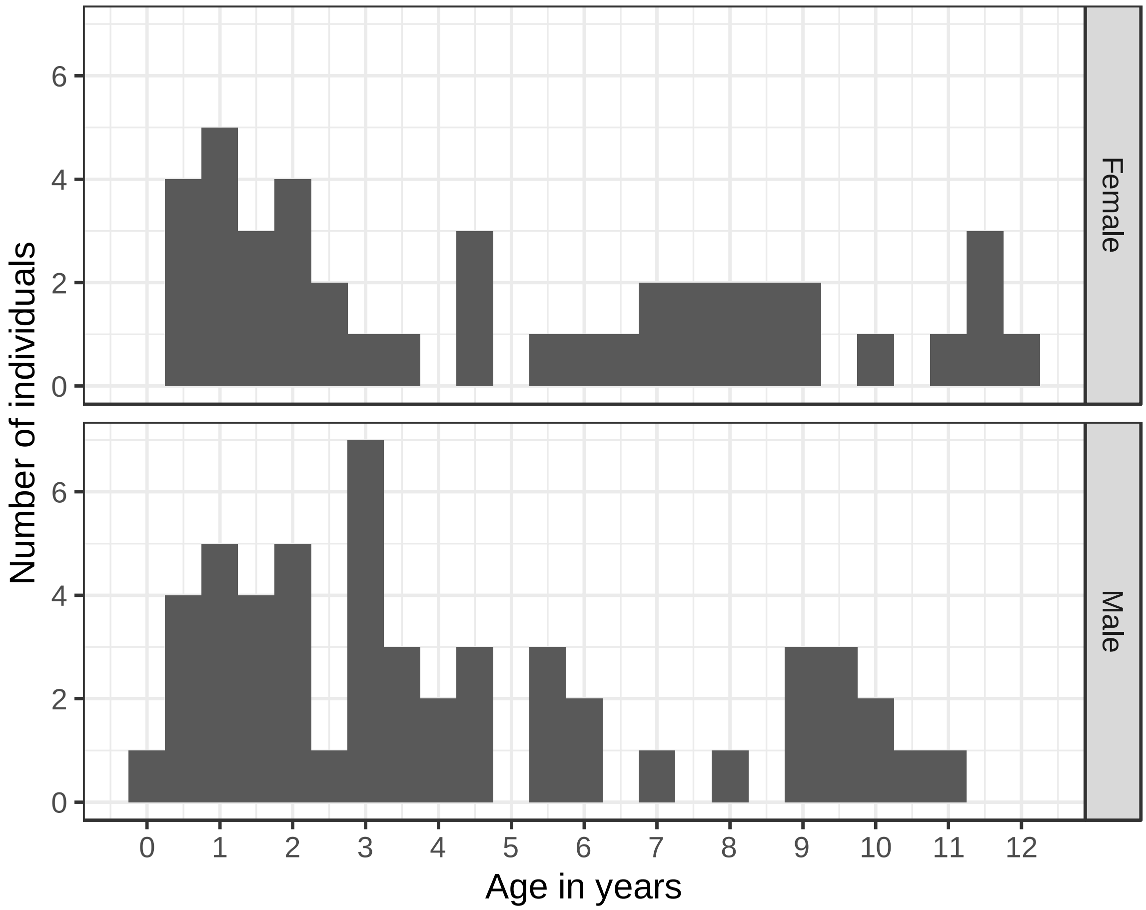
Female
Male
Number of individuals
0
2
4
6
0
2
4
6
0
1
2
3
4
5
6
7
8
9
10
11
12
Age in years

Figure 4.

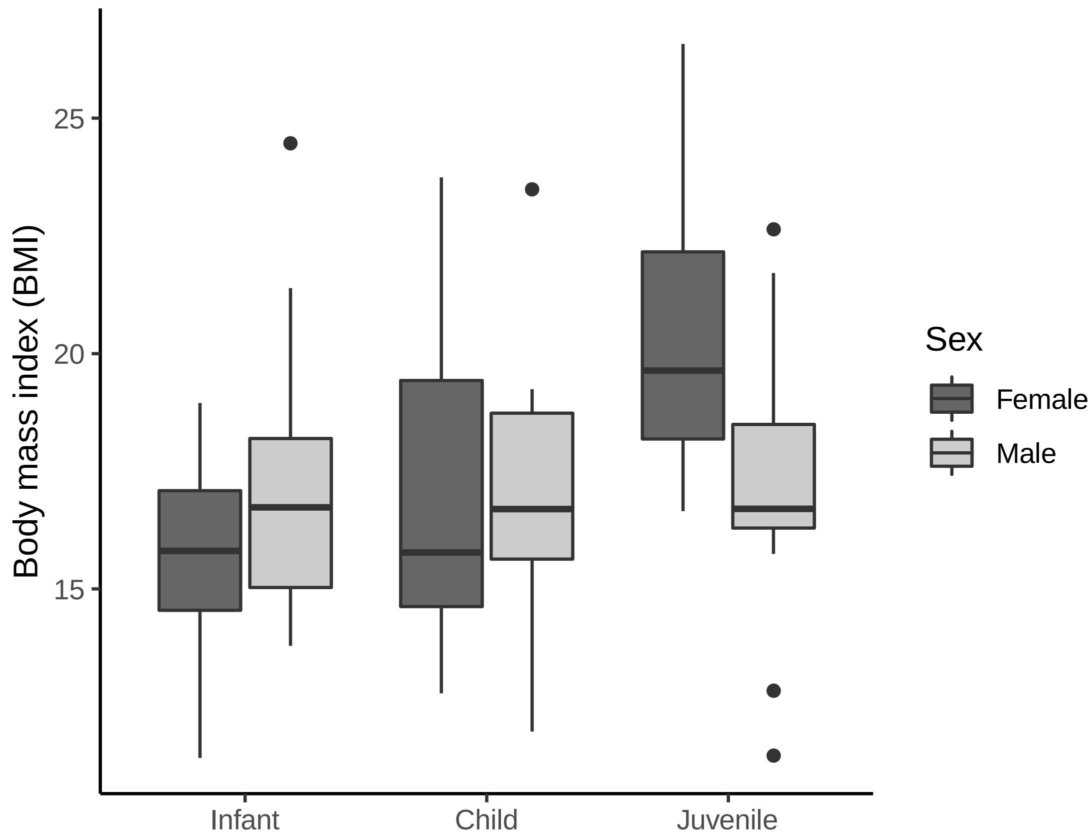

25
20
15
Body mass index (BMI)
Infant
Child
Juvenile
Sex
Female
Male

Figure 5.

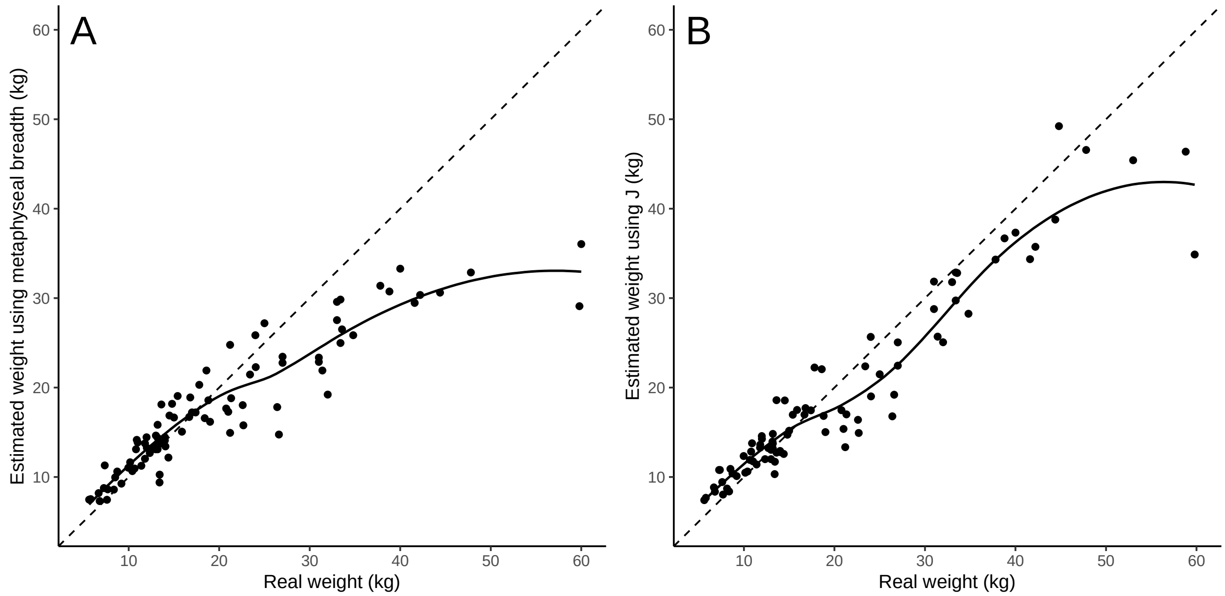
A
B
Estimated weight using metaphyseal breadth (kg)
Estimated weight using J (kg)
Real weight (kg)
Real weight (kg)
10
20
30
40
50
60

Figure 6.

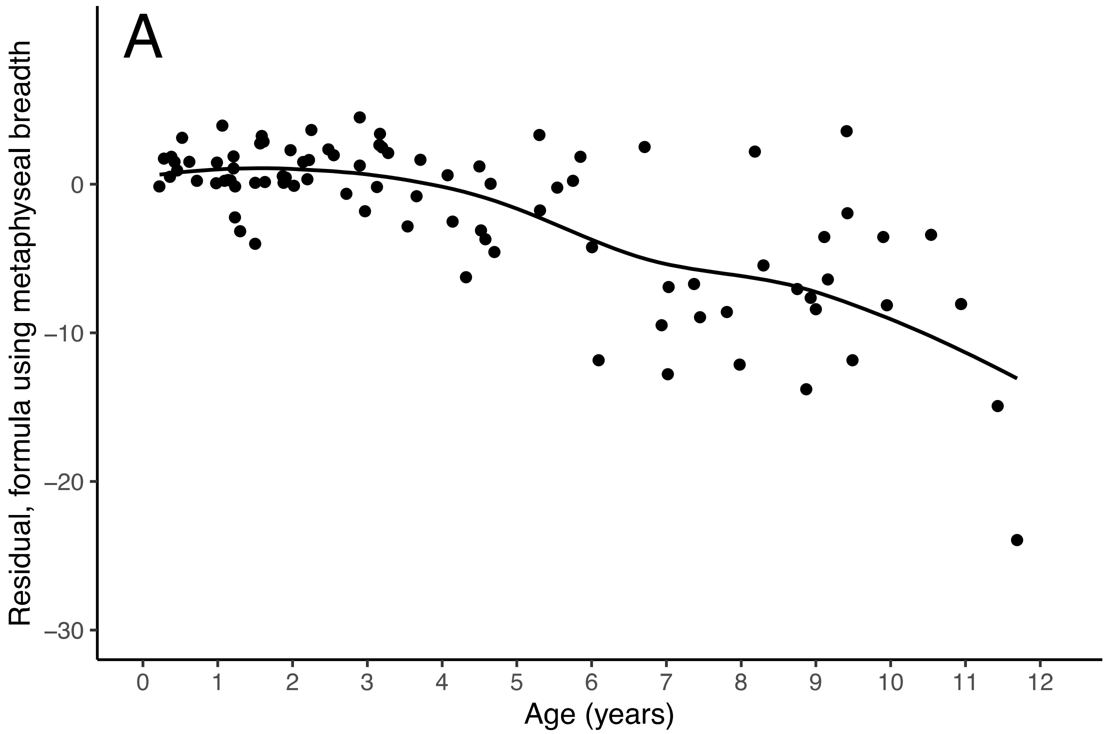

A
Residual, formula using metaphyseal breadth
0
−10
−20
−30
0 1 2 3 4 5 6 7 8 9 10 11 12
Age (years)

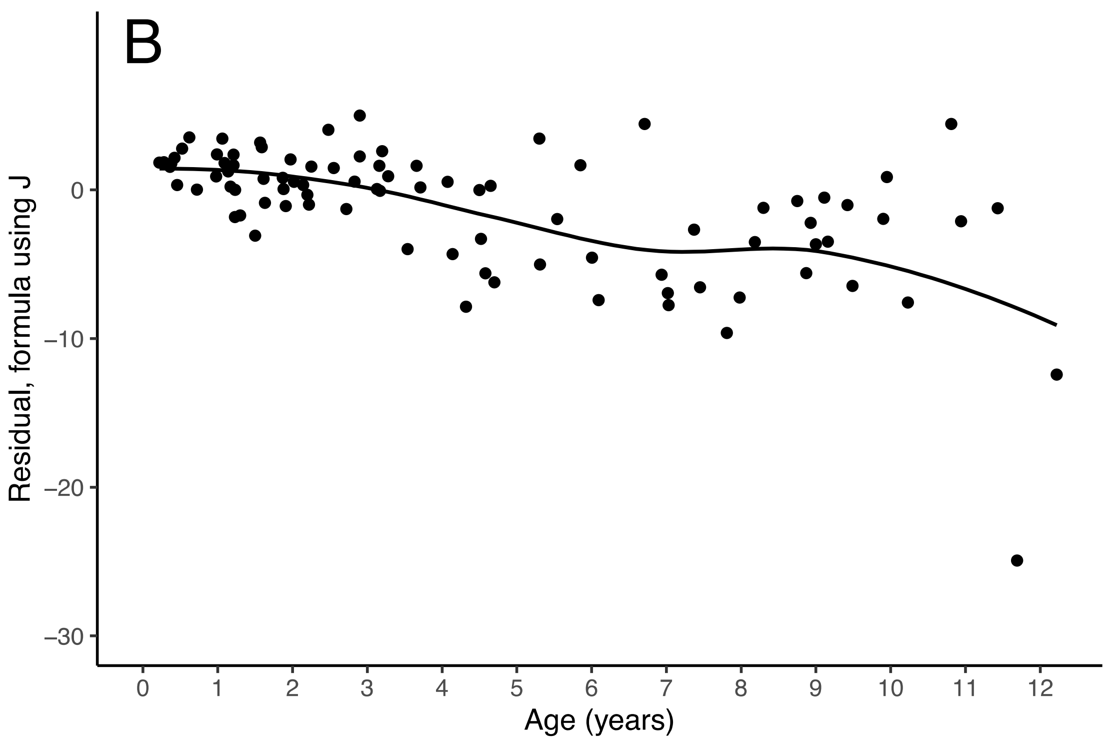

B
Residual, formula using J
0
−10
−20
−30
0 1 2 3 4 5 6 7 8 9 10 11 12
Age (years)